Colloid Polym Sci 275:930–937 (1997)

ORIGINAL CONTRIBUTION

S. Banerjee
V.T. John
G.L. McPherson
C.J. O'Conor
Y.S.L. Buisson
J.A. Akkara
D.L. Kaplan

Polymer microsphere and polymer-ferrite nanocomposite preparation by precipitation from water-in-oil microemulsions

Received: 18 February 1997
Accepted: 30 April 1997

S. Banerjee · Dr. V.T. John (✉)
Department of Chemical Engineering
Tulane University
New Orleans, LA 70118, USA
E-mail: vj@mailhost.tcs.tulane.edu

G.L. McPherson
Department of Chemistry
Tulane University
New Orleans, LA 70118, USA

C.J. O'Connor · Y.S.L. Buisson
Department of Chemistry
University of New Orleans, LA 70148, USA

J.A. Akkarra · D.L. Kaplan
U.S. Army Soldier Systems Command
Natick, MA 01760, USA

Abstract A simple method to encapsulate intramicellar solutes (enzymes, nanoparticles) in polymer microspheres is described. The method involves dissolving a polymer in a minimum amount of solvent. The polymer solution is then added to a large volume of a nonsolvent system containing bis(2-ethylhexyl)sulfosuccinate (AOT) reversed micelles. Immediate precipitation of the dissolved polymer takes place. The precipitation results in the formation of stable microparticles ~ 0.1–$1\ \mu m$ in diameter. There is a direct correlation between the internal voidage of the particles and the water content of the micelles. Precipitation also leads to encapsulation of intramicellar solutes, resulting in the formation of microspherical composites.

Key words Encapsulation – polyphenol – w/o microemulsion – magnetic microspheres

Introduction

The interaction between organized surfactant assemblies and polymers is an area of great interest from both scientific and industrial perspectives [1]. Aqueous solutions of such systems have been studied extensively [2]. Nonaqueous systems, however, have received limited attention [3]. The present work reports the use of water-in-oil microemulsions (also known as reversed micelles) as a nonsolvent medium for polymer precipitation. We have recently established that it is possible to dissolve a presynthesized polymer (poly(4-ethylphenol), PEP) in a solvent and precipitate it in spherical morphology, using a water-in-oil microemulsion as the nonsolvent [4]. The practice of dissolving a polymer in a minimal amount of solvent and then adding it to a large amount of nonsolvent to effect almost immediate precipitation of the dissolved material is well known in the chemical literature [5]. While the use of nonsolvent typically involves a single homogeneous phase, Chang has reported the use of surfactant-free water-in-oil emulsions as the nonsolvent for the synthesis of polymer microcapsules [6]. While a number of generic methods exist for fabricating microspheres [7], precipitation using a complex nonsolvent, i.e. a three-component water-in-oil microemulsion is a new technique and perhaps has some unique features. One of these as described here, is the fact that the internal voidage of the microspheres can be controlled easily by changing the water content of the micelles. A second remarkable feature of precipitation is the fact that intramicellar solutes (e.g. biomolecules such as proteins and enzymes and nanoclusters solubilized in the water pools of the reverse micelles) become trapped in the precipitating polymer matrix. Thus, in addition to microsphere formation, such precipitation can be used as a microencapsulation method. This may lead to the

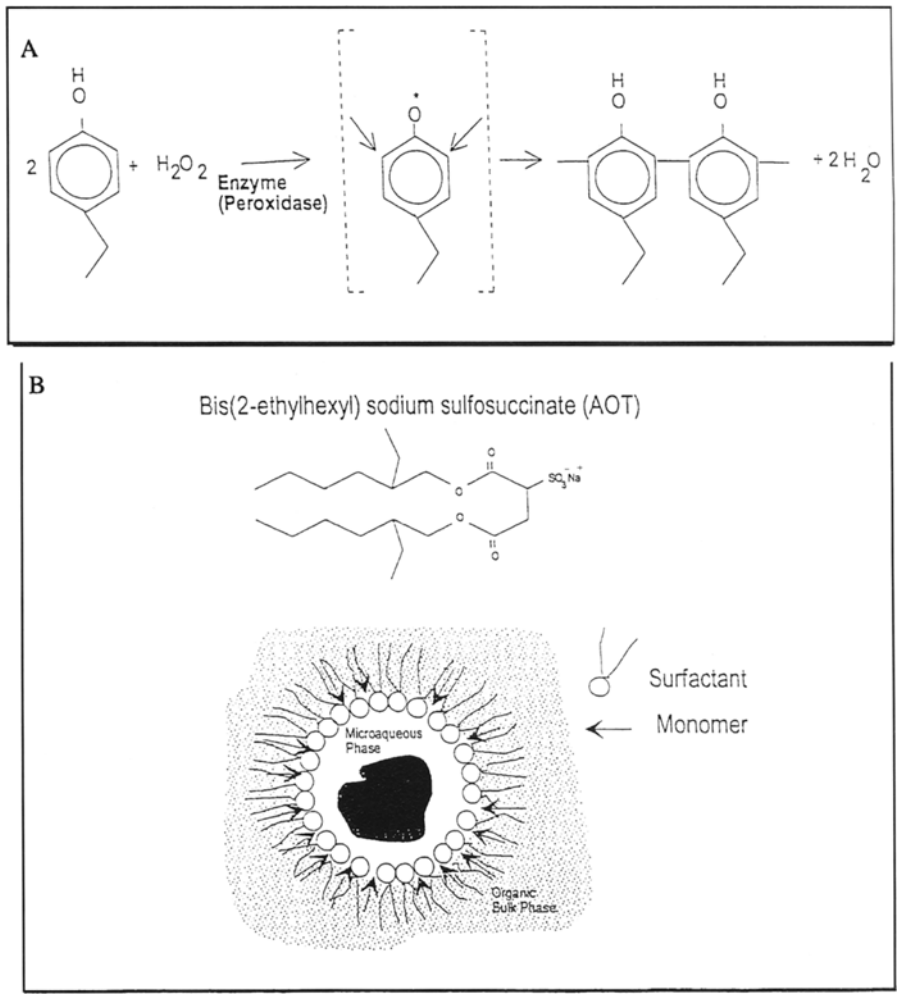

Fig. 1 Schematic of the enzyme-catalyzed polymerization reaction in reversed micelles (A) Simplified mechanism. (B) The enzyme is resident in the water core of the reversed micelles. The monomer is surface active and partitions to the water–oil interface

formation of novel materials where the encapsulate confers its specific property to the composite.

In this paper we report details on such microencapsulation, including a systematic study of the influence of the water content of the microemulsion on the morphology of the precipitated polymer. As an example of microencapsulation, we report the encapsulation of superparamagnetic ferrite nanoparticles in the polymer.

Experimental section

All chemicals were purchased from Sigma-Aldrich (St. Louis, Mo) in analytical grade purity. The surfactant used was bis(2-ethylhexyl)sodiumsulfosuccinate (NaAOT). The bulk organic phase was isooctane. The polar solvent used for dissolution of the polymer prior to reprecipitation was acetone. The specific polymer used here was poly(4-ethylphenol) which was synthesized using an oxidative enzyme, horseradish peroxidase, in the microstructured media of water-in-oil microemulsion [8]. This is an ideal medium to enzymatically synthesize polyphenols, since the microaqueous phase sustains enzyme solubility with activity retention, while the monomers partition to the oil–water interface through hydrogen bonding with the surfactant [8]. Figure 1A illustrates a simplified representation of the condensation of 4-ethylphenol to the polymer. Figure 1B illustrates the chemical structure of the surfactant and monomer partitioning to the interface. The polymer that is formed in the reaction, precipitates out, allowing for easy recovery from the micellar system. The recovered polymer was washed several times with isooctane to remove the traces of adsorbed surfactant, dried and stored for future use. The polymer is amorphous at room temperature, has negligible solubility in water and in aliphatic hydrocarbons (hexane, isooctane, etc.). It is moderately soluble in CCl_4 and chloroform, and highly soluble in polar solvents (acetone, THF, DMSO, etc.). The polymer has an average

Colloid & Polymer Science, Vol. 275, No. 10 (1997)

molecular weight (M_n) of ~1600 Da (polydispersity index ~1.4), as determined by GPC (polystyrene standards, and elution in a Jordi DVB column using THF as an eluent).

Our experiments described here relate to the dissolution of the polymer in a polar solvent and re-precipitation using a large excess of a reversed micellar solution. We have also used reversed-micellar solution containing ferrite nanoparticles for the synthesis of polymer-ferrite composites. Our results pertain to the morphological and magnetic properties of the nanocomposite that is formed.

In all experiments involving polymer precipitation, the general methodology was kept the same. The presynthesized polymer was dissolved in acetone (0.1 g polymer/ml acetone) (solution A). A second solution (nonsolvent solution B) consisting of the reverse micellar solution at an AOT concentration of 0.5 M and the required w_0 (w_0 is the water to surfactant molar ratio) was also prepared. In specific cases, the solution B also contained the γ-Fe_2O_3 nanoparticles (which was to be entrapped within the precipitated polymer microspheres) as an intramicellar solute.

The synthesis of the γ-Fe_2O_3 nanoparticles was carried out in AOT/isooctane reverse micelles ($w_0 = 10$). Two separate micellar solutions were made containing precalculated amounts of $FeSO_4$ and NH_4OH. The reaction was initiated by adding the NH_4OH reversed micellar solution to the $FeSO_4$ reversed micellar solution. The solution turned deep red in a few minutes. The reaction was allowed to proceed for a few hours [9].

The choice of the polymer/solvent/nonsolvent ternary system is extremely important, since it governs the production of polymer microspheres. Acetone was used as the solvent because it is miscible with isooctane. This allows essentially complete diffusion of acetone into the bulk isooctane phase, inducing the formation of a polymer precipitate which is essentially acetone-free. On the other hand, the choice of a polymer solvent which is immiscible with isooctane would result in the formation of two fluid phases on mixing, with the polymer remaining dissolved in the solvent rich phase. Additionally, in this particular instance, acetone also affects the conformation of the polyphenol chains. In nonpolar solvents (e.g. CCl_4), intramolecular hydrogen bonding generates a coiled polymer conformation. On the other hand, polymer-solvent hydrogen bonding in polar solvents such as acetone leads to a fully open conformation in solution, prior to precipitation [4].

Typically, in all experiments, 1 ml of solution A was added to 20 ml of solution B in small aliquots. The solution B was kept stirred using a magnetic stirrer throughout this process. The clear solution B becomes cloudy immediately after the addition of a drop of solution A, indicating that the dissolved polymer has phase-separated. After the addition is complete, the mixture is kept stirred briefly. The supernatant is then removed, and the polymer washed thoroughly with isooctane, to remove all traces of the surfactant.

It is true that besides the water content of the nonsolvent microemulsion phase, a number of other parameters are expected to play a critical role in deciding the properties of the final precipitate. For example, the rate of injection of the polymer solution, the stirring rate, the nature of the injection solvent, initial concentration of the polymer, all affect the final morphology, particle size and distribution. However, our primary objective here is to demonstrate the general feasibility of the precipitation process to generate microspheres and also to evaluate its potential as a microencapsulation technique. Therefore, the effect of systematically changing the process variables listed above on the outcome of the microprecipitation has not been examined.

A Perkin–Elmer atomic absorption spectrometer fitted with a Fe lamp, was used to determine the ferrite contents in the polymer composite. The morphology of the precipitated polymer was characterized by electron microscopy, using a JEOL 820 Scanning Electron microscope operating at 15–30 kV, and a Phillips 410 transmission electron microscope operating at 80 kV. Aluminium stubs (SEM) and carbon-coated copper grids (TEM) were used to mount the samples. The sample preparation involved redispersing a small amount of the precipitated polymer (washed) into isooctane. For SEM, a drop of this solution was then added to the stub and the solvent was allowed to evaporate under ambient conditions. The sample was then sputter-coated with a 20 nm thick gold layer. For TEM, the grid was placed on a filter paper and a drop of the dilute isooctane dispersion of the polymer was added onto the grid. The sample was then air-dried. The SEM micrographs supply information on the overall topography and surface structure of the sample. In TEM, the contrast translates to differences in local "mass thickness" (thickness × density) [10]. The dark regions correspond to regions of greater mass density.

Results and discussion

Polymer morphology

The research involves the use of polyphenols, and we have specifically used para-substituted polyphenols synthesized enzymatically using an oxidative enzyme, horseradish peroxidase which is solubilized in the water pools of AOT reversed micelles. The enzymatic synthesis of such polymers is very feasible and gram quantities of the polymer can be easily obtained. Enzymatic polymerization leads to coupling of the monomers primarily at positions ortho to

the hydroxyl group (Fig. 1A). The polymers typically have low molecular weight ($M_n = 1600$) and are therefore oligomers or prepolymers having on an average ~ 14 monomeric units. They are insoluble in reversed-micellar solutions and during synthesis in this medium, precipitate out. The polymer recovered after synthesis is washed with isooctane to remove all traces of the surfactant, and is now the presynthesized material.

The technique to prepare microspheres discussed here (see Experimental section) utilizes these presynthesized polymers. Thus, poly(4-ethylphenol) is dissolved in a suitable solvent to destroy all gross traces of morphology. Subsequently, the polymer is reprecipitated by contact with a large excess of a reversed-micellar solution which is a nonsolvent for the specific polymer. The theoretical basis of our technique is relatively simple. A stream of good solvent carrying the dissolved polymer is injected into an agitated volume of nonsolvent. The nonsolvent diffuses into the carrier phase and the carrier solvent counter diffuses into the nonsolvent. The polymer molecules nucleate rapidly and phase-separate.

The use of reversed micelles as a nonsolvent to precipitate polymers, is novel, especially if studied in the applied context of micellar solute encapsulation. The specific polymer used here, poly(*p*-ethylphenol), is also rather interesting since it has amphiphilic properties. In nonpolar solvents (e.g. benzene or CCl_4), at low concentrations, intramolecular hydrogen bonding leads to chain folding and curvature, while in polar solvents (e.g. acetone) the polymer adopts a more open structure due to the dominant solvent-segment hydrogen bonding interactions [4]. More interestingly, the surfactant AOT used to form reversed micelles also interacts with the polymer by hydrogen bonding through the carbonyl and sulfonate proton acceptor groups, although in AOT-isooctane reversed micelles, the interactions are not strong enough to sustain polymer solubility. In AOT–CCl_4 reversed micellar solutions (a solvent for the polymer), perturbations to the AOT C=O frequencies are seen upon dissolving the polymer [4]. The polymer is therefore "sticky" due to its strong tendency to hydrogen bond.

Figure 2 illustrates the morphologies of polymer obtained after precipitation in AOT–isooctane reversed micelles as characterized through scanning and transmission electron microscopy. The micrographs illustrate the change in particle characteristics as the water content in the micelle is varied. The water content is quantified through the water-to-surfactant molar ratio (w_0). As the figure illustrates, finely dispersed spherical particles are observed in each case. The microsphere formation is not particularly noteworthy since it is simply due to surface free energy minimization as a consequence of particle nucleation upon supersaturation when contacted with the nonsolvent. Microspheres can be realized simply through direct precipitation in isooctane, although the particle size is typically larger (> 1 μm) than the microspheres shown in Figs. 2A and 2A′. Particles precipitated using the micellar nonsolvent do not show any appreciable shrinkage upon

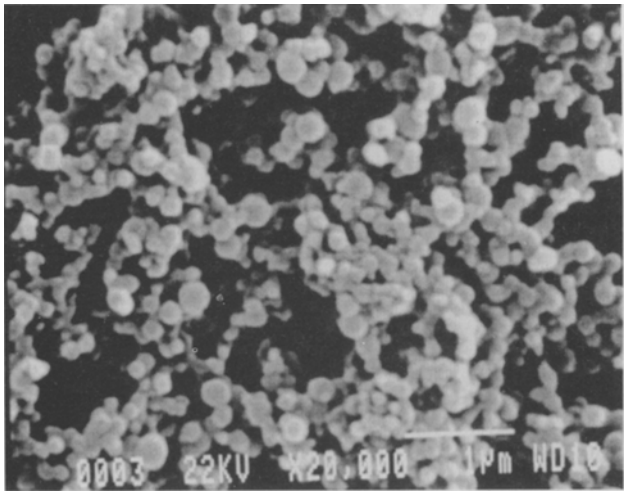

A 1μm

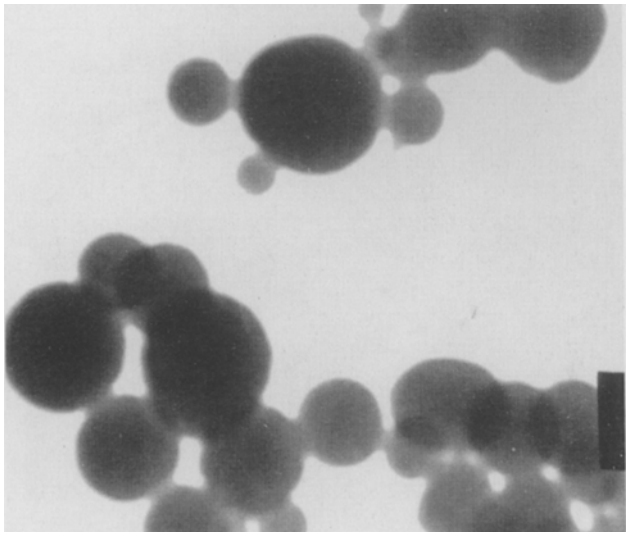

A′ 0.1μm (x 133,000)

Fig. 2 Electron micrographs of the polymer particles when precipitated with (A, A′)$w_0 = 0$, (B, B′)$w_0 = 20$ and (C, C′)$w_0 = 35$ micelles. (A, B, C) refer to scanning electron micrographs while (A′, B′, C′) refer to transmission electron micrographs. A comparison of the particle sizes from the SEM (A) 0.1–0.3 μm, (B) 0.1–0.8 μm, (C) 0.1–1.5 μm clearly indicates particle swelling with use of higher water containing micelles. The TEM illustrates that with increasing water content the internal density of the precipitated particle decreases and at $w_0 = 35$ many particles show a definite core and shell-type morphology

Colloid & Polymer Science, Vol. 275, No. 10 (1997)

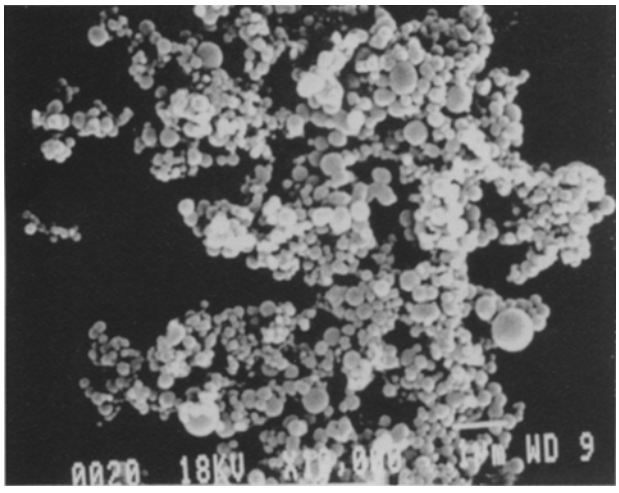

B 1μm

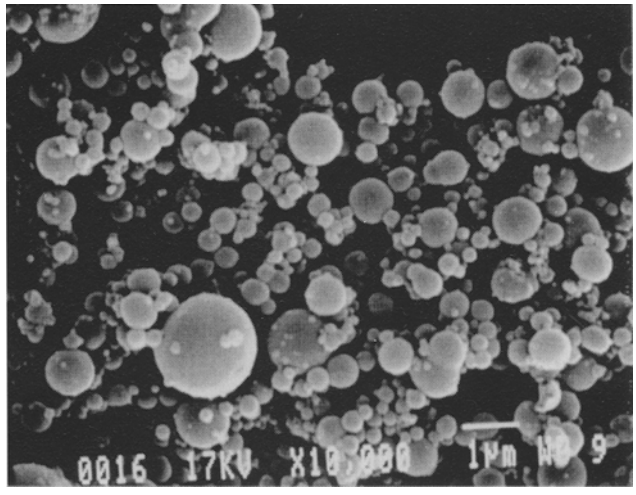

C 1μm

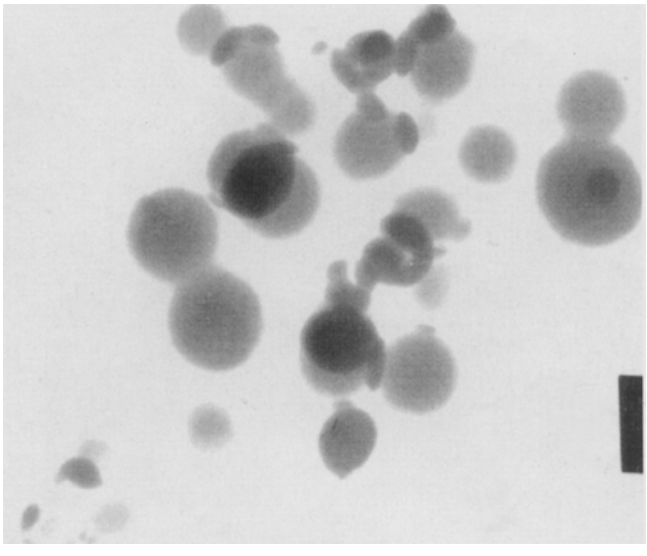

B′ 0.1μm (x 96,800)

Fig. 2B, B′

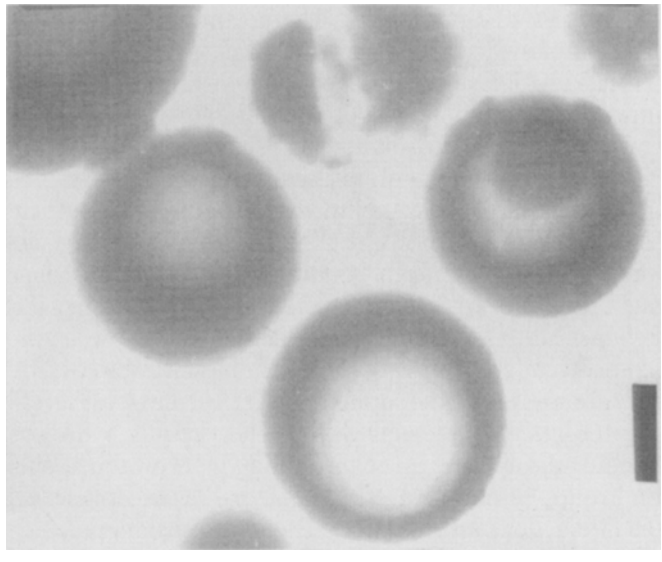

C′ 0.1μm (x 96,800)

Fig. 2C, C′

drying and form loose aggregates, which can be easily redispersed employing mild sonication. Perhaps, the most interesting aspect of the precipitation using the micellar nonsolvent is the role of intramicellar water. As Fig. 2 illustrates, in the presence of water, the polymer particles swell, and seem to have significantly lower internal densities. With $w_0 \geq 30$, over 70% of the particles have a somewhat hollow interior. Such particles are not observed when precipitation is carried out with dry or low-water containing micelles.

These observations are intuitively rationalized. In the case of dry (water-free) micelles, the polymer-acetone solution is initially above its cloud point. Upon contact with the micellar solution, the mutual solubility of acetone and the excess bulk isooctane phase leads to diffusion of the acetone into the bulk hydrocarbon phase. This produces local regions of supersaturation, where a polymer-rich phase begins to separate out. The phase separation probably proceeds via nucleation, which produces droplets of a polymer-rich phase. These droplets are unstable and

coalesce and grow in size. At the molecular level, hydrogen-bonding interactions lead to a combination of chain-folding, chain–chain aggregation and chain interactions with the surfactant. The micelles may additionally serve to compartmentalize the initial seed nuclei. Eventually, the droplets of the polymer-rich phase lose all solvent and precipitate in the nonequilibrium configuration of polymeric microspheres. We note that the microspheres (typically > 0.1 μm) are at least an order of magnitude larger than micelles (less than 0.01 μm).

The formation of the more hollow particles through precipitation in high-water-containing micelles, probably involves more complex interfacial phenomena. Evidently, there is incorporation of water in the precipitating polymer, with retention of water in the microspheres being facilitated by the polar hydroxyl groups of the polymer chains. The hollow sphere morphology may simply be a consequence of the tendency of the incorporated water to segregate from the bulk aliphatic hydrocarbon solvent into the precipitating polymer matrix.

Encapsulation of nanoparticles

The reversed-micellar medium is well suited to the synthesis of inorganic clusters, since the micelles act as nanoreactors restricting growth to the nanometer size range. Thus, superparamagnetic ferrite particles were synthesized in the water pools of reversed micelles using well-established methods of contacting micelles containing the iron (II) sulfate salt with micelles containing ammonium hydroxide (see Experimental section) [9, 11]. The colloidal ferrite nanoparticles stay suspended in the micellar medium. Following ferrite synthesis, polymer precipitation was carried out using the ferrite-containing micellar medium as the nonsolvent. The precipitating polymer entraps the ferrite particles, and depending on the amount of polymer precipitated, over 70% of the ferrite content in the micelles can be entrapped in the polymer matrix.

Figure 3 illustrates the magnetization curves for a polymer–ferrite microsphere composite containing 51.2 mg Fe/g polymer. A SQUID magnetometer was used to determine the magnetic properties. Field-dependent hysteresis loops were generated in the temperature range 2.0–300 K. Typical trends of the magnetic composite are described through hysteresis loops recorded at 100 and 4.5 K. The 100 K loop exhibits no hysteresis, i.e. the magnetization vs field data are perfectly superimpossible as the field is cycled between ± 50 kG. The lack of hysteresis is a characteristic of superparamagnetic particles. Such particles have very small size, and thermal fluctuations are sufficient to overcome the anisotropy barrier, allowing magnetization to spontaneously reverse direction. At a lower temperature

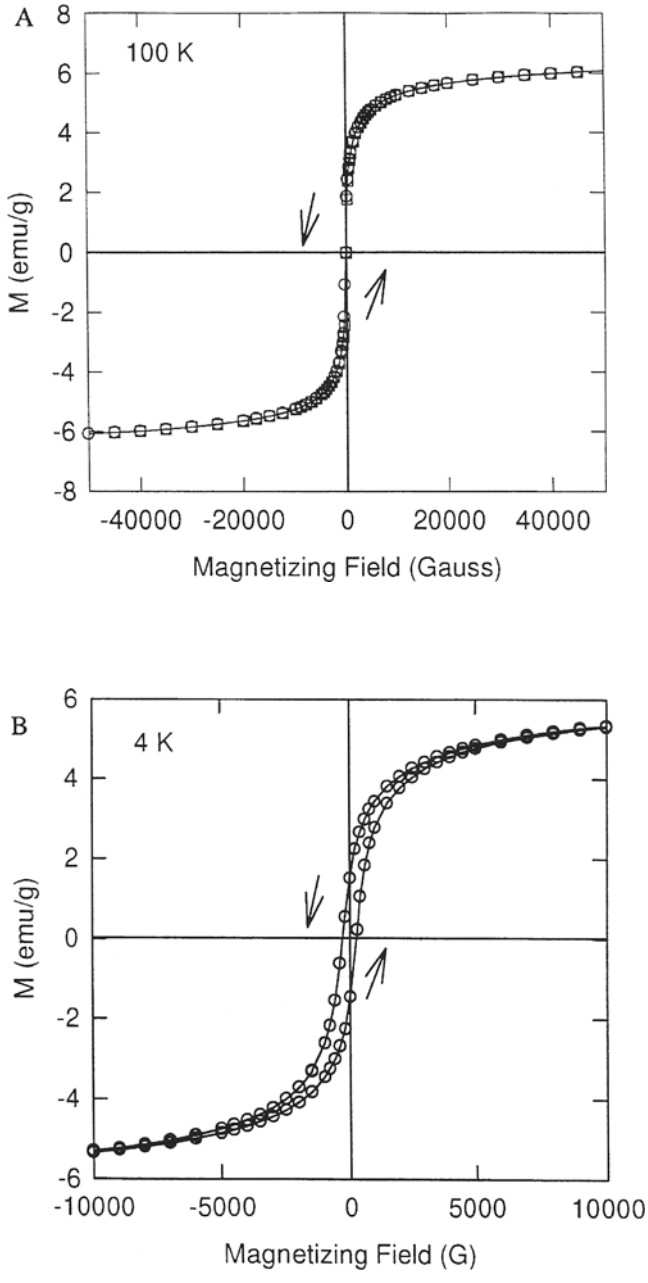

Fig. 3 (A) Magnetization curves for the composite (polymer–ferrite) at 100 K. The sample does not show any hysteresis. (B) The Magnetic hysteresis loop of the same sample measured at 4.5 K. At this low temperature, the sample begins to some hysteresis with coercivity $H_c \sim 300$ G. The presence of low-temperature hysteresis together with the absence of hysteresis at higher temperatures confirms the superparamagnetic nature of the polymer–ferrite composite

of 4.5 K, however, the loop does exhibit hysteresis. The presence of low-temperature hysteresis is due to the freezing of magnetic dipoles. X-ray diffraction analyses indicate broad peaks due to the nanometer size of the ferrite particles, but with distinct features at 2θ values of

Colloid & Polymer Science, Vol. 275, No. 10 (1997)

35.6° and 62.9° attributed to the presence of maghemite (γ-Fe_2O_3) [12].

At 50 kG, the polymer-Fe_2O_3 composite has a magnetic saturation moment of 5.76 emu/g. With 5.2% Fe or 8% γ-Fe_2O_3 (wt%), the calculated saturation moment for the γ-Fe_2O_3 particles is 72 emu/g, which fits reasonably well with the bulk saturation moment of 76.0 emu/g for maghemite [13].

The slope of the magnetization curves (Fig. 3) near $H = 0$ can be used to estimate the upper bound for ferrite particle size in the composite, through the Langevin function [14].

$$M(T) = M_s[\coth(\mu H/kT) - kT/\mu H] \,. \quad (1)$$

For superparamagnetic particles, the Langevin function describes the relationship between magnetization at a particular temperature ($M(T)$) and the applied magnetic field (H) according to Eq. (1). M_s is the saturation magnetic moment, k is the Boltzmann constant and T the absolute temperature. The above equation can be used to estimate the size of the largest particles present in a sample of nonuniform particle sizes using the equation shown below:

$$d_{\mathrm{mag(max)}} = [(18kT/\pi\rho M_s^2)(\mathrm{d}M/\mathrm{d}H)_{H=0}] \,, \quad (2)$$

where ρ is the density of maghemite (5.07 g/cm^3). Using the value of the measured slope $(\mathrm{d}M/\mathrm{d}H)_{H=0}$ of 6.5×10^{-3} emu/(Gauss g composite) (the limiting slope near the origin was determined from the hysteresis plots by curve fitting the linear portion of the data), the largest magnetic particle size ($d_{\mathrm{mag(max)}}$) is about 6 nm. With an 8% by weight γ-Fe_2O_3 loading in the polymer, there are approximately 10^4 ferrite nanoparticles in polymer microspheres of diameter 0.5 μm. Such polymer–ferrite composites have applications in magnetic separations and magnetic coatings. The ease of functionalization of phenolic groups indicates the possibility of immunoaffinity ligand attachment to the polymer for biochemical separations [15].

Conclusions

We have, thus, established a simple method of microsphere preparation where the internal density of the microspheres can be varied. Additionally, the technique can also be used for the microencapsulation of intramicellar solutes. In contrast to traditional composite preparation, where the microsphere is first prepared and the inorganic clusters subsequently synthesized within the pores of the microspheres [16], the technique described here is more of a ship-in-a-bottle approach to entrapping ferrite nanoparticles in nucleating polymer particles. While this paper has dealt with the encapsulation of ferrites, it is also possible to encapsulate enzymes that are previously solubilized in the water pools of the micelles. When enzyme encapsulation is carried out, particularly with the higher water content micelles that lead to the swollen microspheres, the resulting polymer–enzyme composite is catalytically active [4]. The rather high polydispersity of the swollen microspheres, could be a deterrent to applications requiring monodispersity. However, the ability to manipulate particle size and internal density may lead to interesting polymer–nanoparticle and polymer–enzyme composites. Although we have used enzymatically synthesized polyphenols, it should also be possible to use commercially available linear, phenolformaldehyde polymers [17] since the hydrogen bonding interactions of these materials should be similar to the polymer used here [18].

Acknowledgements Financial support from the National Science Foundation and the US Army is gratefully acknowledged.

References

1. Nagrajan R, Harold M (1985) In: Mittal KL, Fendler EJ (eds) Solution Behaviour of Surfactant-Theoretical and Applied Aspects. Plenum Press, New York; Sun F, Ruckenstein E (1993) J Appl Polym Sci 48:1279; Qutubuddin S, Lin CS, Tajuddin Y (1994) Polymer 35:4606
2. Goddard ED, Anathapadmanabhan KP (1993) Interactions of Surfactants with Polymers and Proteins. CRC Press, Boca Raton
3. Steiber F, Eicke H-F (1996) Colloid Polym Sci 274:826; Bakeev KN, Shu YM, Zezin AB, Kabanov VA, Lezov AV, Mel'nikov AB, Kolomiets IP, Rjumtev EI, MacKnight WJ (1996) Macromolecules 29:1320; Luisi PL, Scartazzini R, Haering G, Schurtenburger P (1990) Colloid Polym Sci 268:356
4. Banerjee S, Premchandran R, Tata M, John VT, McPherson GL, Akkara J, Kaplan D (1996) Ind Engg Chem Res 35:3100
5. Aubert JH, Sylvester AP (1991) Chemtech 8:20; Leroux JC, Alle'mann E, Doelker E, Gurney R (1995) Eur J Pharm Biopharm 41:14; Dixon DJ, Johnston KP, Bodmeier RA (1993) AIChE J 39:127; Lele AK, Shine AD (1992) AIChE J 38:742
6. Chang MS (1964) Science 146:524
7. Wilcox DR, Berg M (1995) Mater Res Soc Symp Proc 372:3; Esumi K, Eshima S, Murakami Y, Honda H, Oda H (1996) Colloids Surf 108:113; Tamai H, Sumi T, Yasuda H (1996) J Coll Interf Sci 177:325; Biggs S, Hill A, Selb J, Candau F (1992) J Phys Chem 96:1501; Atik SS, Thomas JK (1991) J Am Chem Soc 103:4259; Candau F (1995) Macromol Symp 92:169
8. Rao M, Gonzalez RD, John VT, Kaplan D, Akkara J (1993) J Biotechnol Bioeng 41:531; Karayigitoglu C, Kommareddi N, John V, McPherson G, Akkara J,

Kaplan D (1995) Mater Sci and Eng C2:165; Akkara JA, Ayyagari M, Bruno F, Samuelson L, John VT, Karayigitoglu C, Tripathy S, Marx KA, Rao DVGLN, Kaplan D (1994) Biomimetics 2:331; Premchandran RS, Banerjee S, Wu X-K, John VT, McPherson GL, Akkara J, Ayyagari M, Kaplan D (1996) Macromolecules 29:6452

9. Kommareddi N, Tata M, Karayigitoglu C, John VT, McPherson GL, Herman MF, Lee YS, O'Connor CJ, Akkara J, Kaplan D (1996) Chem Mater 8:801
10. Sawyer LC, Grubb DT (1987) Polymer Microscopy. Chapman and Hall, New York
11. Lopez-Quintela MA, Rivas JJ (1993) Colloid Interface Sci 158:446; Moumen N, Pileni MP (1996) Chem Mater 8:1128
12. Powder diffraction file (PDF) 39-1346, from the ICDD Database – International Center for Diffraction Data, Newton Square, Pennsylvania
13. Bidan G, Jarjayes O, Fruchart JM, Hannecart E (1996) Adv Mater 6:152
14. Yaacob II, Nunes AC, Bose A, Shah DO (1995) J Colloid Interface Sci 171:73
15. Olsvik O, Popovik P, Skjerve E (1994) Clin Microbiol Rev 7:43
16. Ugelstad J, Soderberg L, Berge A, Bergstrom J (1983) Nature 303:96
17. Kopf PF (1985) Encyclopedia of Polymer Science and Engineerig, Vol 11. Wiley, New York
18. Cairns T, Eglinton G (1962) Nature 196:535